

RSC Advances



This is an *Accepted Manuscript*, which has been through the Royal Society of Chemistry peer review process and has been accepted for publication.

Accepted Manuscripts are published online shortly after acceptance, before technical editing, formatting and proof reading. Using this free service, authors can make their results available to the community, in citable form, before we publish the edited article. This *Accepted Manuscript* will be replaced by the edited, formatted and paginated article as soon as this is available.

You can find more information about *Accepted Manuscripts* in the [Information for Authors](#).

Please note that technical editing may introduce minor changes to the text and/or graphics, which may alter content. The journal's standard [Terms & Conditions](#) and the [Ethical guidelines](#) still apply. In no event shall the Royal Society of Chemistry be held responsible for any errors or omissions in this *Accepted Manuscript* or any consequences arising from the use of any information it contains.

Cite this: DOI: 10.1039/c0xx00000x

www.rsc.org/xxxxxx

PAPER

Polyaniline Nanotubes with Rectangular-Hollow-Core and its Self-assembled Surface Decoration: high conductivity and dielectric properties

Pradip Paik,* Ramesh Manda, Chandar Amgoth, K.Santhosh Kumar

Received (in XXX, XXX) Xth XXXXXXXXX 20XX, Accepted Xth XXXXXXXXX 20XX

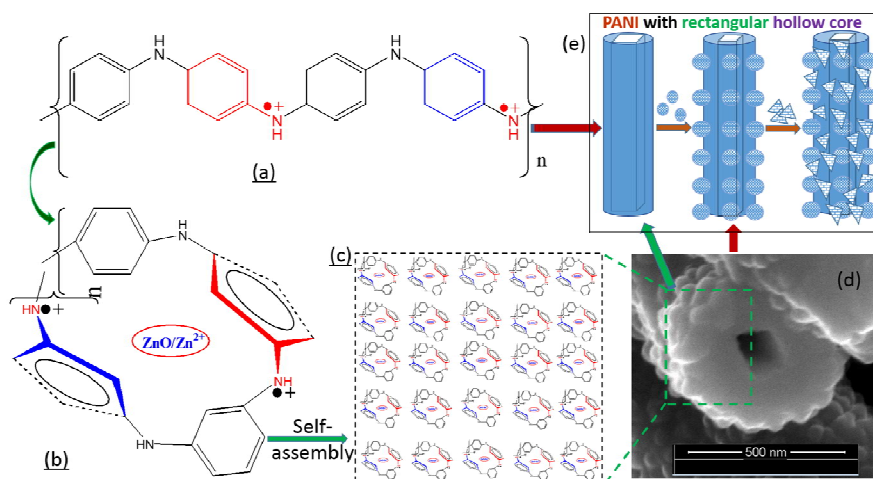
DOI: 10.1039/b000000x

Polyaniline(PANI) nanotubes with a rectangular hollow core and decorated outersurface-wall with self-assembled nanobeads and triangular flakes of PANI have been synthesized in the presence of ZnONPs by sonochemical approach. This is the first example of formation of well-defined hollow PANI nanotubes with rectangular hollow interior. The hollow PANI nanotubes have an average length of ca. 10 μ m and a hollow core with rectangular geometry. Nanobeads of PANI with diameter ca. 50 nm have been decorated/self-assembled on the surface of the outer wall of rectangular hollow PANI nanotubes to obtain a “Dates-tree-body-like” 3D structure. The crystal structure has been characterized through XRD. The conduction bands and electronic environment have been confirmed through Raman, FT-IR, UV-Vis-NIR, XPS and EPR. Impedance measurements of rectangular hollow PANI nanotubes demonstrates its higher electrical conductivity $\sigma = 1.1 \pm 0.1 \times 10^{-4}$ S/m to $3.0 \pm 0.23 \times 10^{-3}$ S/m and dielectric properties depending on the frequency range compared to the PANI particles synthesized in presence of H⁺ and solid PANI fibres. The PANI nanotubes with such a novel rectangular hollow core structure with surface decorated texture is a unique type of nanostructure and that can be used in various conductive polymer based device applications.

1 Introduction

Since the date of discovery in 2001 by Nobel Prize winners Shirakawa, MacDiarmid, and Heeger,¹ the conducting polymer has become a powerful platform for its potential applications in erasable information storage, shielding of electromagnetic interference, radar-absorbing materials, sensors, indicators, actuators, rechargeable batteries, non-linear optical devices, antistatic coatings, light emitting diodes,¹⁻³ including drug delivery^{4,5} and energy storage devices.^{6,7} Conducting polymer

nanofibers have attracted researchers because of its better performances¹⁻⁷ with respect to the bulk counter parts of the same.^{8,9} In our recent published work we reported on the enhancement of physical properties of the nematic liquid crystal (LC) by doping of conductive PANI nanofibers which can be used for magnetically-steered-LC-PANI-nanofibers switch.⁹ To date, many attempts have been made in modifying nanoparticles/nanofibers of polymeric (organic)/inorganic materials by introducing porosity through template



Schematic I (a) Structure of conducting emeraldin salt of PANI, (b) possible rearrangement of PANI backbone (c) self-assembly of PANI in presence of ZnO/Zn²⁻, (d) cross section view of rectangular hollow core and (e) step-wise decoration of PANI with rectangular hollow core.

synthesis,¹⁰ conjugating organic moieties by molecular imprinting (MI),¹¹ coatings with metal nanoparticles¹² etc. in structure that could impart additional functionality to the solid nanostructures, such as selective sensing, optical activity etc.. Sensing properties based on conductivity of polymer nanofibers show promising potential applications in industrial and biomedical applications which include clinical assaying, detection of explosive, chemicals and hazard monitoring.¹² However, their selective detection efficiency is not up to the mark or not satisfactory and moreover it depends on the working conditions like temperature, partial pressure and concentration of the molecules under detection and on the structural alignment of the nanofibers and on the conductivity. 1D conducting polymer nanofibers can be synthesized in many routes such as insoluble hard (e.g., zeolites),¹⁴ soluble soft templating (e.g., surfactants/micelles),^{15,16} seeding¹⁷ and biomolecules¹⁸ which can orchestrate the growth of the 1D nanostructure of the nanofibers but all of them are with solid core or with a circular hollow core. Moreover, the use of conducting polymer is strongly associated with the limiting factors, such as oxidation states, surface textures and morphology, internal structure (like solid or hollow etc.), alignment of the backbone chains, extent of doping with ionic solids, space charge polarization and on the extent of its free electron hopping. PANI usually synthesized by chemical oxidation polymerization of aniline in aqueous solution in the presence of strong acid (pH < 2) in the presence of a strong oxidant ammonium persulfate (APS).¹⁹ PANI nanotubes with circular hollow core can also be synthesized by chemical oxidation in the presence of various inorganic acids and sulfonic acids,²⁰ organic acids,²¹ polymeric acids,²² sulfonated CNTs²³ and dendrons.²⁴ Synthesis of PANI nanotubes with circular hollow core in the presence of TiO₂ has also been reported²⁵. PANI exists in various acid-base and redox forms and substantially their chemical and physical properties depend on their oxidation states. Only the emeraldin salt form (Schematic-1a) of PANI is conducting in nature ($\sigma \sim 10^{-3}$ S/m).²⁶

Herein this work, we report about an innovation of nanoparticles based synthesis method of PANI 1D nanotubes with rectangular hollow interior and surface decorated 3D architecture of nanotubes having very high electrical conductivity and dielectric properties. According to this new procedure, we took ZnO nanoparticles as template in a homogeneous mixture of highly pure aniline in water and performed acid catalyzed sonochemical polymerization. We are able to create a well-defined 1D PANI with rectangular hollow interior along the centre of each fiber under controlled conditions. By controlling the sonochemical reaction conditions, the surface of the PANI tubes has been decorated with spherical PANI nano beads and subsequently architected stepwise with triangular shaped PANI flakes in in-situ conditions. Finally a "Dates-tree-body-like" 3D structure has been designed which are high conducting compared to the solid PANI fibers and PANI nanoparticles. Similarly, we have performed the sonochemical reaction in H⁺ in the presence of Au nanoparticles with equimolecular weight in two different batches and it never formed triangular hollow nanostructure of PANI. The results have been compared with the solid nanofibers of PANI and PANI nanoparticles.

In an earlier work, I and co-researchers have reported on the

formation of microtubes of β -peptide tetramer (trans-(S,S)-aminocyclopentanecarboxylic acid tetramer) having rectangular cross-section (sub-micrometre) by the evaporation induced self-assembly method.²⁷ To the best of our knowledge present work is the first report on polyaniline nanotubes with a rectangular hollow interior and decorated outer surface wall with self-assembled PANI nanobeads and triangular flakes which have been synthesized in presence of ZnONPs by sonochemical approach. Further, this work has been focused on the study of the physical properties such as crystal structure, conductivity and dielectric properties of polyaniline nanotubes with a rectangular hollow interior. The results are very interesting from the application point of views.

2. Experimental

2.1. Materials and Reagent

Aniline (>99.5% Sigma-Aldrich), Ammonium persulphate (APS, NH₄S₂O₈, >98.5%, Sigma), HAuCl₄ (99.999%, Aldrich), Sodium borohydride (NaBH₄, >99%, Sigma) ZnO Nanoparticles (<50 nm diameter, 97%, Aldrich), were purchased and used as received without further purification.

2.2. Synthesis of functionalized polyaniline nanotubes (hollow and surface decorated)

2.2.1. Synthesis of Au Nanoparticles

A 90 ml (0.1 mM) solution of HAuCl₄ was prepared. Aqueous NaBH₄ (10 mL, 0.1 g) was immediately added to the above solution and the stirring was continued for 1 h. The solution turned into light brown colour with the addition of NaBH₄ solution. The reaction was continued overnight to reach completion, resulting in a red-wine colour. The Au solution was dialyzed against deionized water for 24 h in a 12.5 kDa dialysis membrane, with intermittent change of water to purify it and lyophilized to obtain dry powder which was readily dispersible in water.

2.2.2. Sonochemical synthesis of functionalized polyaniline nanofibers in the presence of Au

PANI was synthesized by an aqueous solution polymerization method. A typical synthesis method is as follows: 0.373 gm (4 mmol) aniline was mixed in 20 ml of deionized water in which 0.01 mg of Au nanoparticles (dia-10-15 nm) was added and sonicated it for 30 sec in ice bath to form a homogeneous mixture. A fresh solution of ammonium persulphate (APS, 0.9 gm in 2 ml ice water) and a pre-cooled 10 ml HCl (1M) were added rapidly into the premixed aniline-Au solution. Then the mixture was sonicated for 5 sec in an ice bath and subsequently kept it at 0°C for 24 hrs. The crude product was dialysed for 24 hrs against deionized water until a neutral solution was obtained. The dialysis assisted in the removal of chloroaurate and other ions. Purified PANI was then lyophilized to obtain dry powder which is readily redispersible in water. This is a solid (not hollow) powder and black in colour and designated as PANI@AuNPs/Au⁺³

2.2.3. Sonochemical synthesis of polyaniline nanotubes with

rectangular hollow core in the presence of ZnO

Polyanilin nanofibers in presence of ZnO: A similar procedure was followed to achieve PANI using ZnO (as it was prepared in the presence of Au NPs). A brief synthesis method is as follows: 0.373 gm (4 mmol) aniline was mixed in 20 ml of deionized water in which 0.01 mg of ZnO nanoparticles (dia~30-40 nm) was added and sonicated for 30 sec at 0°C. An APS solution (0.9 gm in 2 ml ice cold water) and a pre-cooled 10 ml HCl (1M) were added rapidly into the premixed aniline-ZnO solution. Then the mixture was sonicated for 5 sec in ice bath and subsequently kept it at 0°C for 24 hrs. The crude product was dialysed against deionized water until a neutral solution was obtained. The dialysis assisted in the removal of Zn⁺², Cl⁻¹ and other ions. Then the purified PANI was lyophilized to obtain dry powder which is readily dispersible in water. This powder obtained is hollow nanofibers, black in colour and designated as PANI@ZnO-NPs/Zn⁺².

Functionalization and decorated polyaniline nanotubes prepared in presence of ZnO NPs: In the second stage, 100 mg PANI (prepared with ZnO) was taken in 50 ml deionized water. Then 1 mmol aniline was added followed by a desired amount of HCl (1M) was added to make it 1:1 [aniline] and [HCl] solution. Then required amount (0.25 gm) of APS was added (molar ratio of [ASP] and [aniline] is ~1:2). Then the reaction mixture was stirred at 75°C in water bath and kept for 10 min for uniform temperature distribution throughout the reaction mixture followed by sonication for 5 sec. Then APS was dissolved and the solution turned into deep green to black. Then the reaction vessel was kept in a closed chamber at 0°C without agitation for 24 hrs. Then it was dialysed against deionized water until a neutral solution was obtained. Purified functionalized PANI was then lyophilized to obtain dry powder. These hollow PANI nanofibers are decorated with flakes and is black in colour and designated as PANI@ZnO-NPs/Zn⁺².

Similarly PANI nanoparticles were prepared without the presence of any other metal salt or nanoparticles other than H⁺ and APS and the sample is designated as PANI0.

2.3. Characterizations

The high resolution images were acquired with HRTEM (JEOL JEM-2100 electron microscope) using an accelerated voltage of 200kV. High resolution focused ion beam (FIB) images were acquired using a FEI Helios 600 system using an accelerated voltage of 5kV. We used a BRUKER AXS D8 ADVANCE Diffractometer (using CuK α λ =1.5418 Å radiation) operating at 40kv/40mA, with a graphite reflected beam monochromator and variable divergence slits for powder X-ray diffraction analysis. Data were collected from 10 to 60° (2 θ) with a resolution of 0.02°. The FT-IR spectra were recorded with a VARIAN spectrophotometer at room temperature with KBr pellets. Thermogravimetry Analysis (TGA) measurements were performed with ThermoONIX Gaslab 300 TGA instrument from 30-1000 °C in N₂ atmosphere. In order to detect the free radicals present in the sample the electron spin resonance (EPR) spectroscopy measurements were performed on a Bruker EPR 100d X-band spectrometer (ν =9.77GHz) with a 100KHz magnetic field modulation (ER083CS), Raman spectra for polyanilin nanofibers were recorded on a JobinYvon Horiba

Raman System. The 632.8 nm line of a He-Ne laser is used as the excitation source, focused to a 1-2 μ m spot size. The UV-Vis-NIR spectra were recorded on a CARY 100 Scan UV-Vis-NIR spectrometer. The oxidation state of the polyaniline samples were investigated by X-ray photoelectron spectroscopy (XPS) measurements on a KRATOS AXIS HS spectrometer using Al KR radiation. The C 1s (binding energy 284.6 eV) peak was chosen as a reference line for calibration of the energy scale. The bulk conductivity of the polyaniline samples were determined by impedance measurements in the frequency range of 25 kHz to 100 Hz

3. Results and Discussions

Size and Morphology: Schematic-1 is showing a possible mechanism for the formation of PANI nanotubes with rectangular hollow interior. Fig.1(A)-(C) show the FIB micrographs for PANI nanotubes with rectangular hollow interior at various magnifications, synthesized by polymerization of aniline in acidic conditions (H⁺) with templating the ZnO-NPs at 0°C temperatures and designated as PANI@ZnO-NPs/Zn⁺² since ZnO NPs become colourless in HCl solution and the following ionic dissociation occurs: ZnO \rightarrow Zn⁺². The details of the synthesis method of PANI@ZnO-NPs/Zn⁺² nanotubes are explained in the experimental section. In order to understand the detailed architecture of the PANI@ZnO-NPs/Zn⁺² nanotubes, HRTEM experiments were employed at various magnifications, Fig. 1(D)-(F). Both FIB and HRTEM investigations revealed that the PANI@ZnO-NPs/Zn⁺² nanotubes are hollow in nature. Microscopy analysis as well ensured that the PANI@ZnO-NPs/Zn⁺² nanofibers have a rectangular hollow core structure with an average geometrical dimension of the core being ~112nm x ~100nm with a wall thickness of ~120 nm. The average length of the PANI@ZnO-NPs/Zn⁺² nanotubes has been found to be ~10 μ m with an average outer diameter of ~350 nm. FIB inspection revealed that the surfaces of the rectangular hollow PANI@ZnO-NPs/Zn⁺² are decorated with the spherical PANI nano beads. The beads are spherical in shape and the diameter is about 50 nm. These PANI@ZnO-NPs/Zn⁺² nanotubes were taken for further stepwise decoration on the surface with extended flakes in stereo space.

Fig. 2(A)-(C) are showing a clear change in morphology and surface decoration and their gradual change in the number density of the functionalized nano beads and flakes. To understand the stepwise decoration of PANI@ZnO-NPs/Zn⁺² nanofibers by polyaniline flakes, we performed three individual batches of reactions, Batch-1: only 1 mmol of aniline was taken with a required amount of ASP and HCl, where the molar ratios of [aniline] and [HCl], and [ASP] and [aniline] were kept 1:1 and 1:2, respectively. Batch-2: 50 mg PANI@ZnO-NPs/Zn⁺² nanotubes was taken with a 1.5 mmol of aniline and required amount of HCl and ASP were added to it, where the molar ratios of [aniline] and [HCl], and [ASP] and [aniline] were kept in 1:1 and 1:2, respectively. Batch-3: 50 mg dried and purified sample from Batch-2 was taken with a 1.5 mmol of aniline with required amounts of HCl and ASP to make the molar ratio of [aniline] and [HCl] to 1:1, and molar ratio of [ASP] and [aniline] to 1:2. All the reactions were carried out at the same condition at 0°C without agitation for 24 hrs. For Batch-1 reaction, only flakes are

formed (Fig. S1). For Batch-2 reaction, flakes are decorating the surface of PANI@ZnO-NPs/Zn²⁺ nanotubes (Fig. 2B). The population density of the flakes on the surface of rectangular hollow PANI@ZnO-NPs/Zn²⁺ is found to be less. For Batch-3 reaction, flakes are decorating on the surface of PANI@ZnO-NPs/Zn²⁺ nanotubes (Fig. 2C) and the number of flakes on the surface of PANI@ZnO-NPs/Zn²⁺ tubes is relatively high compared to the sample obtained from Batch-2 reaction. This clearly indicates that on increasing the aniline amount in decoration process, the surface morphology of the rectangular hollow PANI@ZnO-NPs/Zn²⁺ nanofibers is regulated by the additional number of flakes. In fact the flakes have grown on the surface of hollow PANI@ZnO-NPs/Zn²⁺ nanotubes.

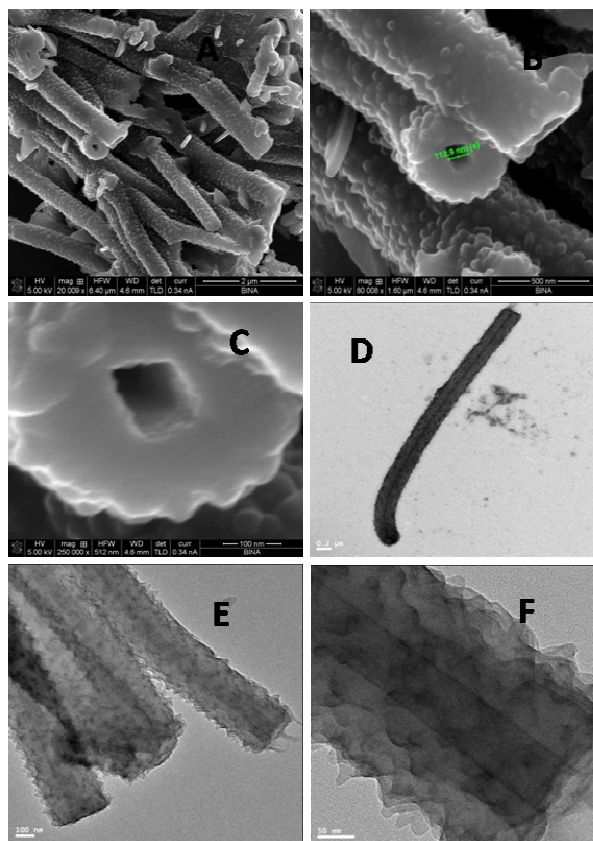


Fig. 1 (A), (B) and (C) FIB images; (D), (E) and (F) HRTEM images of PANI nanotubes with rectangular hollow interior synthesized in the presence of ZnO NPs.

Earlier the a number of formation mechanism of nanofibers of conducting polymers is reported by a group of researchers.^{15-18,28-29} Polyaniline nanostructure such as wires/-nanofibers/-rods/-tubes can be synthesized by introducing 'structural directors', such as soft templates (e.g., surfactants, micelles),^{15,16} organic dopants,¹⁷ biomolecules¹⁸ etc., which can organize the growth of the nanofibers but none of their hollow structure is rectangular in shape. Recently, it is also found that the introduction of small amount of dimers/oligomers into the polymerization reactions can control the growth of the fibers.²⁸ The amount of mer units, oxidizer (APS) and catalyst (H⁺) present in the reaction process can regulate whether it will form fibers or flakes.²⁹ However, to the best of our knowledge the formation of nanotubes with

rectangular hollow interior with surface engineered and decorated by flakes by systematic steps is an advancement of designing the nanostructure of conductive polymers and has not been reported earlier. Therefore, nanostructures have been decorated by introducing ZnO/Zn²⁺ in the reaction mixture. Without the introduction of Au/Au³⁺ or ZnO/Zn²⁺ in reaction mixture it forms the spherical shaped submicron sized PANI particles with nanopillar on the surface of the spheres even all the other reaction conditions have been kept same (PANI0, see Fig. S2).

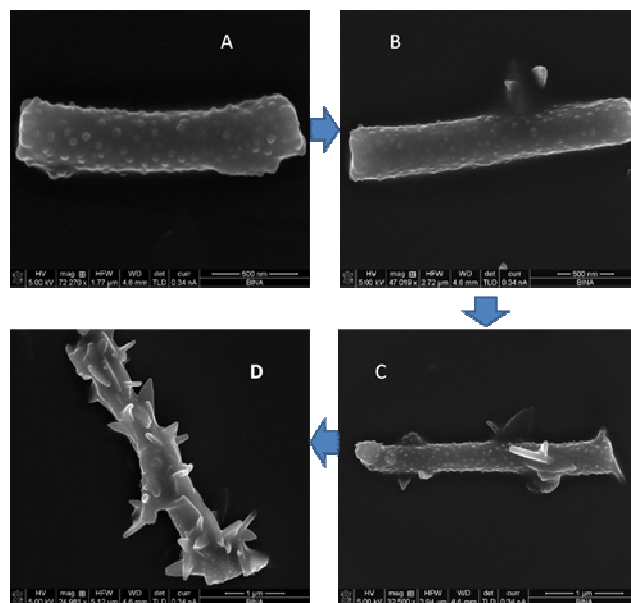


Fig. 2 FIB images of hollow PANI nanotubes (A) Surface decorated by spherical nano bead of PANI (sample-1 for decoration, synthesized with ZnO NPs), (B-D) surface decorated by PANI nano flexes (sample-2 for decoration synthesized with ZnO NPs, step-2), and (C) surface decorated by PANI nano flexes (dense flexes) synthesized with ZnO NPs, (from A to D sequential steps).

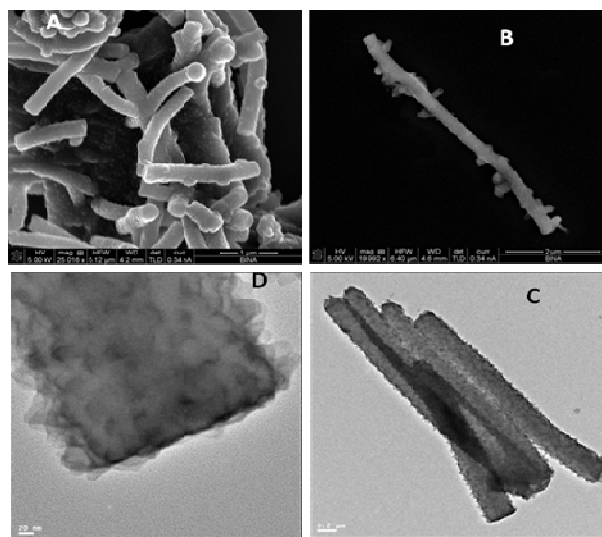


Fig. 3 (A) and (B) FIB micrograph and (C) and (D) HRTEM of PANI nanofibers synthesized in presence of Au NPs.

Fig.3(A) and 3(B) show the FIBmicrographsfor a branch ofPANI nanofibers and single nanofiber, respectively, which have been synthesized by polymerization of aniline in acidic condition (H^+) with templating the Au NPs at $0^\circ C$. A colloidal solution of Au NPs was added in 1(M) HCl solution, the red-pink colour of the solution becomes colourless due to the electronic transition: $Au^0 \rightarrow Au^{+3}$ and hence we have designated the final product as PANI@AuNPs/ Au^{+3} .

In order to understand the construction of the PANI@AuNPs/ Au^{+3} nanofibers, HRTEM was employed relatively at lower and higher magnifications, Fig. 3(C) & (D), respectively. Both FIB and HRTEM insight that the PANI@AuNPs/ Au^{+3} nanofibers are solid, i.e., obtained polyaniline fibers do not have any hollow interior. Microscopy analysis as well revealed that the PANI@AuNPs/ Au^{+3} nanofibers have an average length of about $10 \mu m$ with an average diameter of ~ 250 nm. The idea of adding Au nanoparticle in the synthesis is to get the highly oriented solid PANI in metallic ionic medium (Au^{+3}).

Formation mechanism of rectangular hollow PANI@ZnO-NPs/ Zn^{+2} nanotubes: The difference in the formation of functionalized PANI nanofibers/tubes in our methods from the other methods is that, it is a two-step process: first step is the atomization of aniline at $0^\circ C$ temperatures to form PANI molecules followed by the crystal growth at the same temperature with ZnO/ Zn^{+2} system (Fig. 2). Secondly, we allowed growing the PANI flakes on the surface of the rectangular-hollow-core PANI nanotubes at $0^\circ C$. If the polymerization of aniline is allowed to form PANI at the temperature range of $75-80^\circ C$ followed by crystal growth then the PANI chains are not able to grow effectively to form 1D nanofibers due to the high solubility of aniline at such a higher temperature.²⁹

If the polymerization occurs followed by the crystal growth in between $0-5^\circ C$, even then PANI crystal could not grow effectively to a 1D direction. If polymerization is allowed at higher temperature, as example at $75-80^\circ C$ followed by the crystal growth in between $0-5^\circ C$, then it leads to the formation of oriented solid PANI fibers.²⁹ The introduction of small amount of dimers/oligomers into the polymerization reactions can control the growth of the conducting polymer nano fibers.²⁸ When polymerization of aniline in the presence of ZnO/ Zn^{+2} ionic system under ultrasonication is allowed and is combined with crystal growth at $0^\circ C$, then the highly fascinated and oriented PANI 1D nanotubes with rectangular hollow interior are formed in high yield. Whenever we have allowed polymerization of aniline in the presence of Au/ Au^{+3} under ultrasonication followed by the crystal growth at $0^\circ C$, the highly oriented PANI 1-D nanofibers are formed but without any hollow core. There is an obvious question, what is the role of Au/ Au^{+3} or ZnO/ Zn^{+2} ?

We observed that the presence of Au/ Au^{+3} control the high orientation of the PANI fibers and helps the fibers to grow in 1D without forming any hollow structure in the centre of the fibers even all other synthesis conditions maintained same. In absence of any NPs or ions (Au/ Au^{+3} ions or ZnO/ Zn^{+2}) lead to the formation of uncontrolled growth of the fibers with irregular surface morphology. Additionally, polymerization of aniline in presence of ZnO/ Zn^{+2} leads to the formation of PANI nanotubes

with rectangular hollow core and the formation of well-defined rectangular hollow interior of nanotubes of conductive polymer (i.e., PANI) follow the self-assembling intermolecular arrangement mechanism of polymer chains along the longitudinal direction. Although in some cases the formation of micron sized fibers with β -peptide and with other aromatic molecules have been reported but not having hollow-rectangular cross-sectional interior.^{27,30}

It is worth mentioning that the concentration of aniline and H^+ are important parameters to control the growth of polyaniline at $0^\circ C$. When temperature is $0^\circ C$ and the reaction is in progress, the concentration of H^+ in the reaction medium reach to zero at a certain stage and the concentration of polyanilinium salt also decreases or do not form further due to the lack of H^+ ions. This situation leads to the formation of spherical crystal beads of PANI what we are able to create on the surface of PANI. These PANI nano beads induces the self-assembly on the surface of the rectangular hollow tubes as it is observed in Fig. 3(A) in such a fascinating manner that the distance between the beads are almost same. In the present work we are able to create the uniform sized and spherical beads of size around 50 nm in diameter on the surface of the rectangular hollow PANI nanotubes. The nano beads are decorated isotropically due to a stabilized ionic environment of oxidised aniline droplets which have been placed at equal distance on the surface of the fibers. Thus nano beads of PANI are self-assembled on the rectangular hollow PANI tubes.

In the stepwise process for the formation and decoration of flakes on the surface of hollow-rectangular PANI tubes (Fig. 3B and Fig. 3C), it is also observed that the formation of flakes and its morphology also depend on the aniline concentration. Typically, for the formation of PANI flakes and its self-assembly on rectangular hollow tubes the concentration of [aniline]: $[H^+]$ is maintained 1:1 with an aniline concentration of as low as 0.8 mmol. In this work it is observed that the thickness of PANI flakes is ~ 100 nm with triangular shape. All the triangular flakes are self-assembled on the surface of the rectangular hollow PANI tubes in such a fascinating manner that finally it appears like a "Dates-tree-body-like" 3D structure.

In order to assure the molecular structure of the PANI, PANI@AuNPs/ Au^{+3} and PANI@ZnO-NPs/ Zn^{+2} the FT-IR spectroscopy analysis has been performed at room temperature. The FT-IR results of the PANI reveals that the bands at 1573 and 1490 cm^{-1} are attributed due to the deformation (stretching) mode of $-C=C-$ of the quinoids and benzoid rings. The band at 1299 cm^{-1} is assigned to the C-N stretching of the secondary aromatic rings. The band at 1243 cm^{-1} appeared due to the stretching and vibration of the $-C-N-C-$ bonds present in polaron. The band at 1122 cm^{-1} is arisen due to the bending and vibration of $-C-H$ bonds in plane. This bond forms during the protonation of aniline during polymerization and broadens towards the higher wave numbers range beyond 1178 cm^{-1} . The bands at 695 and 1049 cm^{-1} are the results of the outer plane bending of 1,2 rings and 1,2,4 rings, respectively. The peaks in between $800-900$ cm^{-1} appear due to the para substitution of the aromatic rings followed by the polymerization proceed through the head-to-tail mechanism. The quinoid units are converted to benzoid units upon acid protonation of the emeraldine base by a proton induced spin-unpairing mechanism and therefore, no prominent

absorption peak appears at around 1380 cm^{-1} . The protonated emeraldine shows a long absorption tail above 1950 cm^{-1} , and an absorption peak appears around 3250 cm^{-1} , is due to the stretching of N-H bonds. The appearance of intense broad band at 1178 cm^{-1} is associated with the high electrical conductivity and due to the high degree of delocalization of free electron in PANI. The results indicate that the broadening of this peak is more for the PANI0 and PANI@ZnO-NPs/Zn²⁺ compared to the

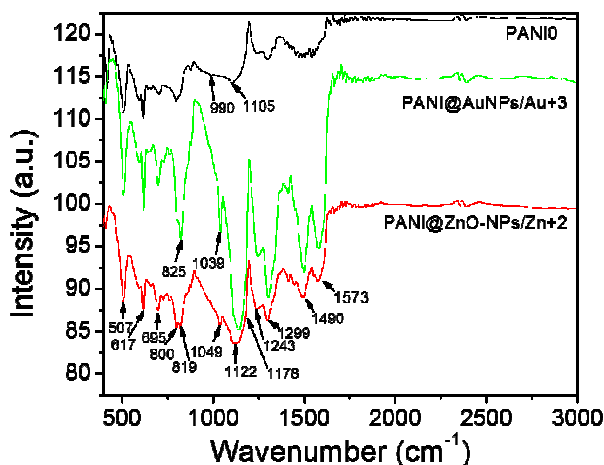


Fig. 4 FTIR spectra for PANI0, PANI@AuNPs/Au³⁺ and PANI@ZnO-NPs/Zn²⁺ showing the molecular structure and chemical bondings responsible for the conductivity.

PANI@AuNPs/Au³⁺. The peak broadening for rectangular-hollow PANI@ZnO-NPs/Zn²⁺ is highest among the three different samples. This is also an indication of lower conductivity of PANI@AuNPs/Au³⁺ compared to the PANI0 and PANI@ZnO-NPs/Zn²⁺. The conductivity value is high for the rectangular-hollow PANI@ZnO-NPs/Zn²⁺ which we have found from the impedance study (discussed in separate section). Additional peaks other than the peaks/bands related to the conductivity are matching with other FT-IR peaks and are the common observation for the PANI backbone structure which usually obtained by the traditional chemical synthesis route mainly acid catalyzed polymerization of aniline.^{31,32}

UV-Vis-NIR absorption spectra of PANI0, PANI@AuNPs/Au³⁺ and PANI@ZnO-NPs/Zn²⁺ were conducted in deionised propanol (Fig. 5). The characteristic peaks for PANI0 appear at 360, 462 and 890 nm (long tail); for PANI@AuNPs/Au³⁺ at 378, 443, and 891 nm (long tail); whereas for PANI@ZnO-NPs/Zn²⁺ the peaks appear at 247, 276, 373, 440 and 885 nm (long tail). The absorption spectra in Fig. 5 shows that the peaks at 247 nm and 276 nm arise due to the $\pi \rightarrow \pi^*$ transition and the polaron band $\rightarrow \pi^*$ transition of PANI rectangular hollow nanofibers (distinct for PANI@ZnO-NPs/Zn²⁺), respectively. The peak arisen at 360-378 nm is due to the $\pi \rightarrow \pi^*$ transition in the benzoid ring of the emeraldine base form of polyaniline.¹⁶ The band in between 440 to 462 nm and the extended broad band starting from 580 to 1400 nm is attributed to the $\pi \rightarrow$ localized polaron band.²⁹ This represents the presence of major conducting form of emeraldine salts of the PANI synthesized with H⁺ catalyst and the conjugation is extended to a long range order. The absorption between 440 to 462 nm and the

extended broad band starting from 580 to 1400 nm is attributed to the $\pi \rightarrow$ localized polaron band for the emeraldine salt is 860 nm for PANI@AuNPs/Au³⁺ and it might be the possible reason for the less conjugation length and hence less conductivity compared to the PANI@ZnO-NPs/Zn²⁺ and PANI0 (absorption band peak at 891 nm and free carrier tail of conjugated electron extended far beyond 1400 nm).^{16,29} This could be the possible reason for the high conductivity for rectangular-hollow PANI@ZnO-NPs/Zn²⁺ and PANI0 compared to the PANI@AuNPs/Au³⁺. Similar results we have found from the impedance study (discussed in the subsequent section). Due to the electron spin-orbital coupling/overlap of the phenyl ring's π electrons and nitrogen lone pairs the extent of conjugation decreases and results in the less conductivity for the PANI@AuNPs/Au³⁺ solid fibers compared to the other two samples (PANI@ZnO-NPs/Zn²⁺ and PANI0).

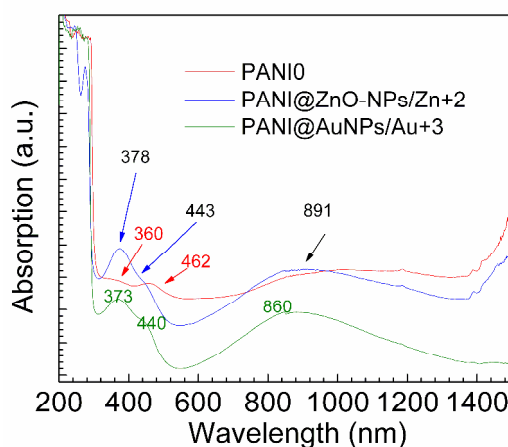
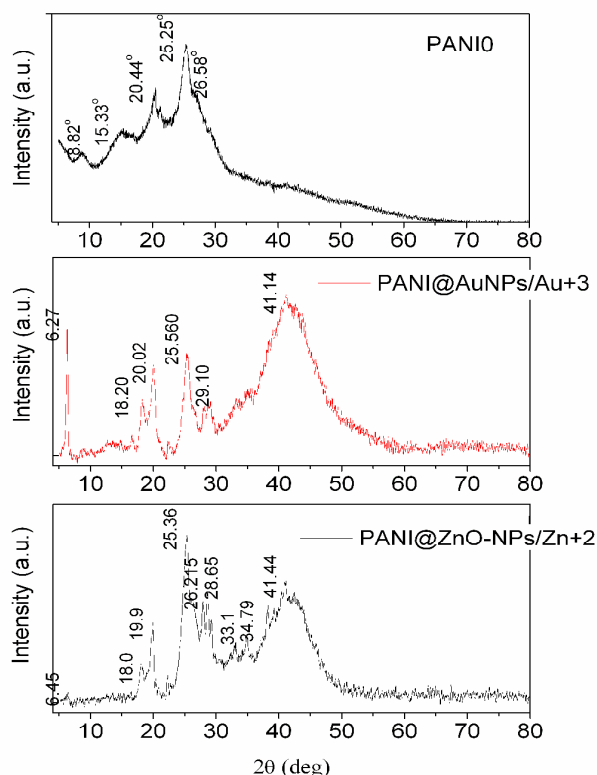


Fig. 5 UV-Vis-NIR spectra for PANI0, PANI@AuNPs/Au³⁺ and PANI@ZnO-NPs/Zn²⁺ showing conduction and non-conduction bands.

The XRD patterns of the PANI0, PANI@AuNPs/Au³⁺ and PANI@ZnO-NPs/Zn²⁺ have been shown in Fig. 6 to distinguish the solid state crystalline structure of the samples. The XRD pattern of the PANI0 shows four distinct peaks at $2\theta = 8.82^\circ$ (d spacing = 10.01), 15.33° ($d = 5.78$), 20.44° ($d = 4.32$) and 25.25° ($d = 4.35$). The peak arisen at 20.44° is due to the periodicity of polymer chains where the PANI chains are arranging parallel to each other. The peaks at $2\theta = 25.25^\circ$ may be attributed due to the periodicity of the polymer chains where the chains are arranged in a perpendicular manner.³³ XRD pattern for the PANI@AuNPs/Au³⁺ shows six distinct peaks at $2\theta = 6.27^\circ$, 18.20° , 20.02° , 25.56° , 29.10° and 41.14° having 'd' spacing of about 14.01, 4.87, 4.43, 3.48, 3.10 and 2.19 Å, respectively. For the PANI@ZnO-NPs/Zn²⁺, eight distinct diffraction peaks appear at $2\theta = 6.44^\circ$, 18.01° , 19.89° , 25.36° , 28.65° , 33.10° , 34.79° and 41.44° with 'd' spacing 13.7, 4.92, 4.46, 3.51, 3.11, 2.70, 2.56, and 2.19 Å, respectively. The peaks at $2\theta \sim 20.44^\circ$ and $2\theta \sim 25.25^\circ$ are the general observation for the PANI, whereas the peak at $2\theta \sim 6^\circ$ for PANI@AuNPs/Au³⁺ and PANI@ZnO-NPs/Zn²⁺ is observed for the highly ordered crystalline structure of PANI.³⁴ Usually, the PANI synthesized by a conventional acid catalysed (H⁺) method do not show any distinct XRD peaks and is amorphous in nature. However, an additional peak for both of PANI@AuNPs/Au³⁺ and

PANI@ZnO-NPs/Zn⁺² is observed at 2θ ~41° due to the very high orientation of PANI chains in long range order. In conclusions, the 1D backbone structure of PANI with very high length/diameter ratio with surface decoration by nano beads and nano flakes (Fig. 1 and Fig. 2) are highly crystalline. In the conventional PANI synthesis method, the aniline monomer reacts with HCl to form aniliniumcation and it is become difficult to crystalline them in aperiodic order on vigorous stirring and produce amorphous aggregate of aniliniumcations. Detail XRD



indexing and results have been calculated³⁵ and represented in Table 1.

Fig. 6 XRD pattern of PANI0, PANI@AuNPs/Au⁺³ and PANI@ZnO-NPs/Zn⁺².

Table 1. Results obtained from the XRD: d-spacing(Å) and (hkl) indexing against 2θ (deg.).

PANI@ZnO-NPs/Zn ⁺²			PANIO			PANI@AuNPs/Au ⁺³		
2θ	'd'	(hkl)	2θ	'd'	(hkl)	2θ	'd'	(hkl)
spacing			spacing			spacing		
6.44	13.7	-	8.82	10.01	-	6.27	14.01	-
18.01	4.92	(002)	15.33	5.78	(101)	18.20	4.87	(110)/ (002)
19.89	4.46	(012)	20.44	4.32	(012)	20.02	4.43	(012)
25.36	3.51	(200)	25.25	4.35	(012)	25.06	3.48	(112)/ (200)
28.65	3.11	(211)				29.10	3.10	(211)
33.10	2.70	(212)				41.14	2.19	(114) (221)
34.79	2.56	(131) (123)						
41.44	2.19	(114) (221)						

Thermal stability of PANI0, PANI@AuNPs/Au⁺³ and PANI@ZnO-NPs/Zn⁺² were checked with TGA (Fig. S3). The thermogram clearly shows that the degradation of all samples occur in three steps. The weight loss at 100°C is due to the moisture whereas all the major weight loss is observed at 300°C. After 500°C the rate of weight loss of PANI@AuNPs/Au⁺³ sample is quite faster with respect to the PANI0, and PANI@ZnO-NPs/Zn⁺². This is due to the wide distribution of the size of the polymer chains. The low molecular weight PANI polymer chain degrades faster on heating. Faster weight loss associated with the low M_w (molecular weight) and it can assume that the electronic conjugation length is also less for PANI@AuNPs/Au⁺³ compared to the other two samples, i.e., PANI0, and PANI@ZnO-NPs/Zn⁺².

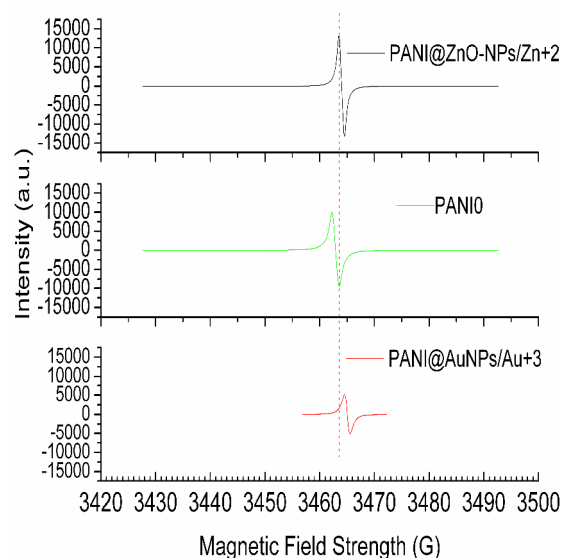


Fig. 7 EPR spectra for PANI0, PANI@AuNPs/Au⁺³ and PANI@ZnO-NPs/Zn⁺².

The conductivity of PANI is strongly associated with its oxidation states. The Raman spectroscopy is very sensitive tool to define the various oxidation states and here we found out the conducting states of novel PANI0, PANI@AuNPs/Au⁺³ and PANI@ZnO-NPs/Zn⁺² samples (Fig. S4). Our PANI samples are found to be a mixture of both its non-conducting emeraldine base and conducting emeraldine salt forms as it has been revealed from the FT-IR and UV-Vis-NIR (Fig. 4 and 5). For PANI0, PANI@AuNPs/Au⁺³ and PANI@ZnO-NPs/Zn⁺² samples, the band appears at 1350 cm⁻¹ because of the presence of conducting emeraldine salt form and thus the PANI fibers forms through the intermediate polysemiquinone radical formation mechanism.³⁶ The peak at 1580 cm⁻¹ appears due to the stretching of -C=C-quinoid consisted with the cross linking for all the synthesized samples.³⁷ But it is very difficult to calculate the extent of the conducting emeraldine salt present in the samples. However, we have confirmed the same from the impedance spectroscopy study.

In order to investigate the free electron responsible for the conductivity of all the PANI samples, EPR experiments were performed apart from the UV-Vis-NIR (Fig. 5). EPR spectra corroborate the presence of radical cations and these are the characteristics for the PANI0, PANI@AuNPs/Au⁺³ and

PANI@ZnO-NPs/Zn²⁺ sample to be conducting (Fig. 7). EPR for PANI0, PANI@AuNPs/Au³⁺ and PANI@ZnO-NPs/Zn²⁺ represent signals at $g = 2.003$. All the samples are showing the similar shape for the spectra, while PANI@AuNPs/Au³⁺ showing the peak broadening and the intensity of the peak decreasing from PANI@ZnO-NPs/Zn²⁺ to PANI0 then to PANI@AuNPs/Au³⁺. The broadening of the peaks in PANI0 and PANI@AuNPs/Au³⁺ are due to the reduction of the diffusion of the unpaired electrons compared to the PANI@ZnO-NPs/Zn²⁺. It is evident that the presence of Na⁺, K⁺, Ca²⁺ or Mg²⁺ in composite system of PANI-zeolite/clays hindered the free-electron's movement.³⁸ Thus the occurrence of Zn²⁺ or Au³⁺ during the synthesis of PANI (and their successive removal by solvent treatments) affects the formation of nanostructure. The complete removal of Zn²⁺ or Au³⁺ is assured by the XPS spectra study and results have been shown in the supporting file Fig. S5 to Fig. S7 and in the supporting Table S1 to Table S3. In conclusions, metal ions are not only hindered the electron diffusion of the PANI (conducting polymers) but it also influences the extent of formation of the emeraldine salts.

The frequency dependant ($f = 0$ to 50 kHz) dielectric properties and electronic conductivity of PANI@ZnO-NPs/Zn²⁺ have been studied and compared with the results of PANI0 and PANI@AuNPs/Au³⁺ with an open circuit potential of zero volt (V) at room temperature (300 K).

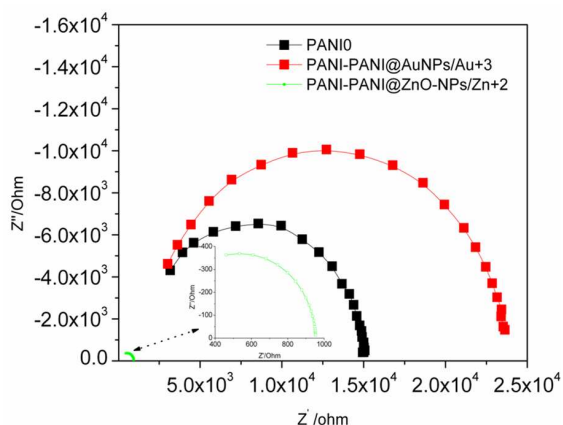


Fig. 8 Cole-Cole plot for the PANI0, PANI@AuNPs/Au³⁺ and PANI@ZnO-NPs/Zn²⁺. Inset is the enlarged view for PANI@ZnO-NPs/Zn²⁺.

Figure 8 shows the Cole-Cole plots for the dielectric relaxation and revealed that the relaxation obeys the cole-cole circular arc law for all three samples, PANI0, PANI@AuNPs/Au³⁺ and PANI@ZnO-NPs/Zn²⁺. The parallel connected R-C circuit was used as an equivalent scheme of the cell. The relative complex dielectric constant, ϵ^* is calculated by eqn. (1-3),

$$\epsilon^* = \epsilon' - i\epsilon'' = \left[\frac{C_p^*}{C_o} \right] \dots \dots \dots (1)$$

with the empty cell capacity C_o . Where,

$$\frac{C_p}{C_o} = \frac{1}{Z'(i\omega)} X \frac{1}{C_o} = \epsilon' \dots \dots \dots (2a)$$

$$\frac{C_p''}{C_o} = -\frac{1}{Z''(i\omega)} X \frac{1}{C_o} = \epsilon'' \dots \dots \dots (2b)$$

$$C_o = \epsilon_o \frac{\pi \left(\frac{D}{2} \right)^2}{d} \dots \dots \dots (3)$$

Our sample cell consists of round parallel plates with diameter D (~10 mm) and spacing $d \sim 0.5$ mm, C_o is calculated by the formula:

The frequency dependent ϵ' (dielectric constant, real part) and ϵ'' (dielectric constant, imaginary part) have been measured and is represented as log-log plot in Fig. 9. ϵ' is determined to be 30 ± 1.5 ($f = 50$ kHz) to 71 ± 2.6 ($f = 500$ Hz) for PANI@ZnO-NPs/Zn²⁺ which is of very high value compared to the PANI0 (minimum 0.6 ± 0.1 , maximum 4.4 ± 0.25) and PANI@AuNPs/Au³⁺ (minimum 0.5 ± 0.1 , maximum 4.7 ± 0.22). Similarly, it is found (Fig. 9) that the frequency dependant ϵ'' is very high for PANI@ZnO-NPs/Zn²⁺ compared to PANI0 and PANI@AuNPs/Au³⁺. There are different mechanisms for the dielectric response and the electrical conduction in polymers/organic materials. The dielectric relaxation at ultra low frequency range (10^{-1} to 10^{-6} Hz) is the result usually from the ionic space-charge polarization³⁹ or from the electrical double layer formation at the electrode.⁴⁰ The ionic space-charge polarization arise due to the long range movements of the impurity ions in the system. In our system the PANI samples are synthesized in the presence of H⁺ catalyst which leads to the formation of emeraldine salts. Whereas Zn²⁺ adds the additional influences in it. None of our samples points for cole-cole plots that were obtained in between 0 to 400 Hz.

Further, based on the imaginary (ac conductance) ϵ'' components of the permittivity (ϵ^*) data, the frequency-dependent ac current conductivity (σ) of the PANI@ZnO-NPs/Zn²⁺, PANI@AuNPs/Au³⁺ and PANI0 have been determined from 400 Hz to 50 kHz (shown in Fig. 10) using the formula (eqn. 4):

$$\sigma = 2\pi\epsilon_o\epsilon''f \dots \dots \dots (4)$$

where, ϵ_o is the dielectric constant of the free space (8.854×10^{-12}). For PANI@ZnO-NPs/Zn²⁺, σ is determined to be $1.1 \pm 0.1 \times 10^{-4}$ S/m to $3.0 \pm 0.23 \times 10^{-3}$ S/m. This value is quite high compared to the σ values obtained for PANI@AuNPs/Au³⁺ ($8.6 \pm 0.43 \times 10^{-6}$ to $2.7 \pm 0.21 \times 10^{-5}$ S/m) and PANI0 ($7.1 \pm 0.31 \times 10^{-6}$ S/m to $9.9 \pm 0.27 \times 10^{-5}$ S/m) at the similar conditions.

Further the frequency depended dielectric loss (dissipation factor) values $\tan(\delta)$ have also been calculated in the same frequency range at room temperature (Fig. 11) and found out that PANI@ZnO-NPs/Zn²⁺ have always a higher value compared to the solid PANI fibers (PANI@AuNPs/Au³⁺) and nanoparticles (PANI0). The Frequency dependence of conductivity of PANI@ZnO-NPs/Zn²⁺ at different temperature have also been measured and it reveals interesting results (Table 2) that with higher temperature conductivity decreases due to the resistance caused by the lattice vibration and disturbance of the electronic resonance/hopping in the PANI backbone is a known factor.

It is evident that the ac current conductivity σ is associated

with the frequency-dependant ionic conductivity (σ_i) and electronic hopping (electronic resonance) conductivity (σ_e), i.e., $\sigma = \sigma_i + \sigma_e$. The frequency-dependant component σ_i is typical for ionic conductivity of liquids.⁴¹ The conductivity of PANI is predominantly associated with the frequency-dependant electronic hopping as it is known, and not due to the occurrences of liquid part in any structural form of PANI (see TGA plot, Fig. S3). Therefore, it is worth mentioning that the high value of frequency-dependent ac current conductivity (σ) of the PANI with rectangular hollow core [PANI@ZnO-NPs/Zn²⁺] is a unique finding

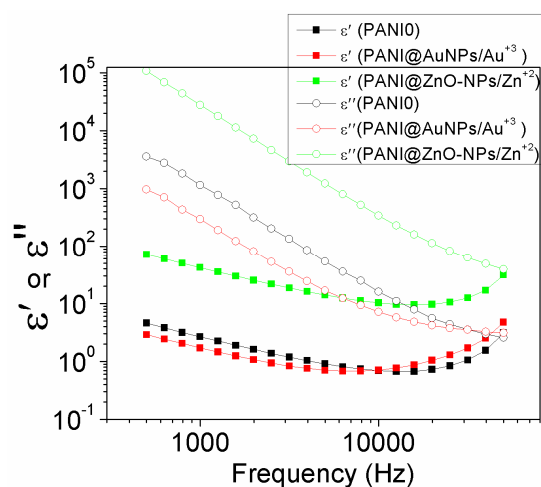


Fig. 9 Frequency dependence of relative dielectric constants ϵ' and the relative dielectric loss ϵ'' for PANI0, PANI@AuNPs/Au⁺³ and PANI@ZnO-NPs/Zn⁺².

Table 2. Frequency dependence of conductivity of PANI@ZnO-NPs/Zn⁺² at different temperature.

Frequency (Hz)	5x10 ²	10 ³	10 ⁴	2x10 ⁴	5x10 ⁴
σ (30°C)	2.98 x 10 ⁻³	1.55 x 10 ⁻³	1.88 x 10 ⁻⁴	1.23 x 10 ⁻⁴	1.10 x 10 ⁻⁴
σ (45°C)	1.07 x 10 ⁻³	8.61 x 10 ⁻⁴	1.09 x 10 ⁻⁴	7.45 x 10 ⁻⁵	7.02 x 10 ⁻⁵
σ (60°C)	6.39 x 10 ⁻⁴	3.36 x 10 ⁻⁴	4.71 x 10 ⁻⁵	3.86 x 10 ⁻⁵	4.37 x 10 ⁻⁵

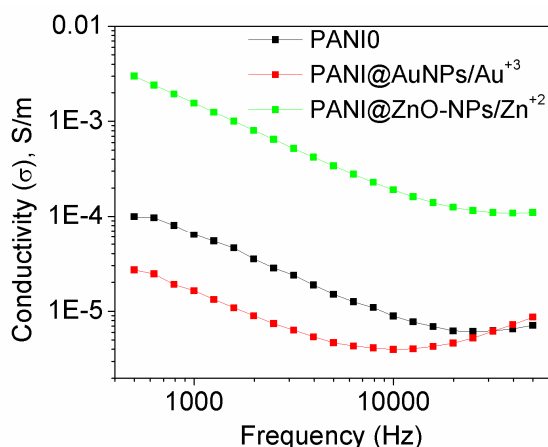


Fig. 10 Frequency dependence of conductivity of PANI@ZnO-NPs/Zn⁺², PANI0 and PANI@AuNPs/Au⁺³.

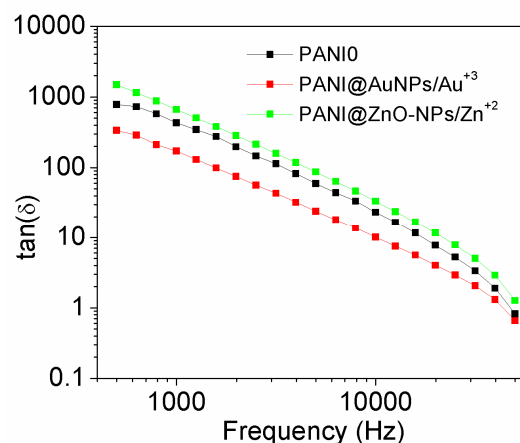


Fig. 11. Frequency dependence of $\tan \delta$ of PANI@ZnO-NPs/Zn⁺², PANI0 and PANI@AuNPs/Au⁺³.

4. Conclusions

In conclusion, we prepared PANI nano tubes with rectangular hollow interior through sonochemical method in the presence of ZnO/Zn⁺² system. This is the first report on the polymer nanotubes with rectangular hollow interior. The outer wall of the rectangular hollow tubes has been decorated with PANI nanobeads and triangular nano flakes by a self-assembly approach to obtain a “Dates-tree-body-like” 3D structure. Frequency dependent ac conductance and the dielectric properties of the rectangular hollow PANI nanotubes have been investigated through the impedance measurements and the excellent enhancement of these properties have been observed compared to the results obtained for solid PANI nanoparticles and solid nanofibers. Therefore, novel rectangular hollow PANI nanotubes with rectangular hollow core with surface decorated nanostructure is a unique nanostructure conducting polymer which can be used in various applications such as for sensing, capacitance, electronic device fabrication etc. However, the mechanistic formation of rectangular hollow core is assumed to occur through a self-assembly of PANI chains. Further detail studies are needed in this direction to understand fully the reason for the formation of rectangular hollow core of PANI. More detail study towards this will be reported elsewhere.

Acknowledgement

This work is supported by the University of Hyderabad (Central University) Start-up Grant (UH/F&A/2011-12/SG) and Department of Science and Technology (DST), India, Fast Track Grant for the Young Scientists (SR/FTP/ETA-00792011)

Notes and references

⁵⁵ School of Engineering Sciences and Technology, University of Hyderabad, Hyderabad 500 046, India. Fax: XX XXXX XXXX; Tel: +91-40-2313 4457; E-mail: ppse@uohyd.ernet.in, paik@uohyd.ac.in, pradip.paik@gmail.com

⁶⁰ † Electronic Supplementary Information (ESI) available: Fig. S1: PANI flakes formed when the molar ratios of [aniline] and [HCl], and [ASP]

- and [aniline] were kept 1:1 and 1:2, respectively (Batch-1); Fig. S2: PANI0 synthesized in H^+ only; Fig. S3: TGA of PANI0, PANI@Au NPs/Au $^{+3}$ and PANI@ZnO NPs/Zn $^{+2}$; Fig. S4: Raman spectra for PANI0, PANI@AuNPs/Au $^{+3}$ and PANI@ZnO-NPs/Zn $^{+2}$; Fig. S5: XPS spectra for PANI@Au NPs/Au $^{+3}$; Fig. S6: XPS spectra for PANI0 and Fig. S7: XPS spectra for PANI@Au NPs/Au $^{+3}$. Table S1, Table S2 and Table S3, the XPS results for PANI@AuNPs/Au $^{+3}$, PANI0 and PANI@Au NPs/Au $^{+3}$ respectively. Supplementary information is available inDOI: 10.1039/b000000x/
- 1 A. J. Heeger, *Angew. Chem., Int. Ed.* 2001, 40, 2591; A. G. MacDiarmid, *Angew. Chem., Int. Ed.* 2001, 40, 2581; H. Shirakawa, *Synth. Met.* 2001, 125, 3.
- 2 M. Angelopoulos, *IBM J. Res. Dev.* 2001, 45, 57; W. A. Gazotti, A. F. Nogueira, E. M. Girotto, L. Micaroni, M. Martini, S. D. Neves and M. De Paoli, *Handbook of Advanced Electronic and Photonic Material: H. S. Nalva (Ed.), Academic Press: San Diego, CA, 2001, Vol. 10, p 53.*
- 3 R. A. Bissell, K. C. Persaud and P. Travers, *Phys. Chem. Chem. Phys.* 2002, 4, 3482.
- 4 S. Geetha, C. R. K. Rao, M. Vijayan and D.C. Trivedi, *Anal. Chim. Acta* 2006, 568, 119.
- 5 P. M. George, D. A. LaVan, J. A. Burdick, C. -Y. Chen, E. Liang and R. Langer, *Adv. Mater.* 2006, 18, 577.
- 6 N. Oyama, T. Tatsuma, T. Sato and T. Sotomura, *Nature* 1995, 373, 598.
- 7 W.-C. Chen and T.-C. Wen, *J. Power Sources* 2003, 117, 273.
- 8 J. Huang and R. B. Kaner, *Angew. Chem. Int. Ed.* 2004, 43, 5817; R. B. Kaner, *ACS Nano*, 2008, 2(9), 1841; H. D. Tran and R. B. Kaner, *Chem. Commun.* 2006, 3915; X. Zhang and S. K. Manohar, *Chem. Commun.* 2004, 2360;
- 9 R. Manda, V. Dasari, P. Sataranaya, N. V. Rasna, P. Paik and S. Dhara, *Appl. Phys. Lett.* 2013, 103,141910.
- 10 P. Paik, Y. Mastai and A. Gedanken, *J. Mater. Chem.*, 2010, 20, 4085; P. Paik, Y. Mastai and A. Gedanken, *Micro. Meso Mater.*, 2010, 129, 82; P. Paik, Y. Mastai and A. Gedanken, *ACS Appl. Mater. Interface*, 2009, 1(8), 1834.
- 11 G. Wulff, *Angew. Chem., Int. Ed. Engl.* 1995, 34, 1812; T. Takeuchi and J. Haginaka, *J. Chromatogr., B: Anal. Technol. Biomed. Life Sci.* 1999, 728, 1; C. Alexander, H. S. Andersson, L. I. Andersson, R. J. Ansell, N. Kirsch, I. A. Nicholls, J. O'Mahony and M. J. Whitcombe, *J. Mol. Recognit.* 2006, 19, 106; A. Thomas and M. Antonietti, *Adv. Funct. Mater.*, 2003, 13, 763; B. Wang, C. Chi, W. Shan, Y.H. Zhang, N. Ren, W. L. Yang and Y. Tang, *Angew. Chem., Int. Ed.*, 2006, 45, 2088; S. Che, Z. Liu, T. Ohsuna, K. Sakamoto, O. Terasaki and T. Tatsumi, *Nature*, 2004, 429, 281; S. Polarz and A. Kuschel, *Adv. Mater.*, 2006, 18, 1206.
- 12 D. Chowdhury, *J. Phys. Chem. C*, 2011, 115 (28), 13554.
- 13 V. Svetlicic, A. J. Schmidt and L. L. Miller, *Chem. Mater.* 1998, 10, 3305; S. Sharma, C. Nirkhe, S. Pethkar and A. A. Athawale, *Sens. Actuators, B* 2002, 85, 131; I. G. Casella, T. R. I. Cataldi, A. Guerrieri and E. Desimoni, *Anal. Chim. Acta*, 1996, 335, 217; G. Li, M. Josowicz, J. Janata and S. Semancik, *Appl. Phys. Lett.* 2004, 85, 1187; M. D. Shirsat, M. A. Banger, M. A. Deshusses and N. V. Myung, A. Mulchandani, *Appl. Phys. Lett.* 2009, 94, 083502; S. Virji, J. D. Fowler, C. Baker, J. Huang, R. B. Kaner and B. H. Weiller, *Small* 2005, 1, 624; J. Huang, S. Virji, B. H. Weiller and R. B. Kaner, *J. Am. Chem. Soc.* 2003, 125, 314; J. Wang, S. Chan, R. R. Calson, Y. Luo, G. Ge, R. S. Ries, J. R. Heath and H. -R. Tseng, *NanoLett.* 2004, 4, 1693.
- 14 C. G. Wu and T. Bein, *Science*, 1994, 264, 1757; Martin, C. R. *Acc. Chem. Res.* 1995, 28, 61.
- 15 Z. X. Wei, Z. M. Zhang and M. X. Wan, *Langmuir*, 2002, 18, 917; H. J. Qiu, M. X. Wan, B. Matthews and L. M. Dai, *Macromolecules* 2001, 34, 675; Z. M. Zhang, M. X. Wan and Y. Wei, *Adv. Funct. Mater.* 2006, 16, 1100; J. Jang and H. Yoon, *Langmuir*, 2005, 21, 11484; M. G. Han and S. H. Foulger, *Small*, 2006, 2, 1164; W. B. Zhong, S. M. Liu, X. H. Chen, Y. X. Wang and W. T. Yang, *Macromolecules*, 2006, 39, 3224;
- 16 P. Anilkumar and M. Jayakannan, *Macromolecules*, 2007, 40, 7311.
- 17 X. Y. Zhang, W. J. Goux and S. K. Manohar, *J. Am. Chem. Soc.* 2004, 126, 4502; X. Y. Zhang and S. K. Manohar, *J. Am. Chem. Soc.*, 2004, 126, 12714.
- 18 Z. W. Niu, M. A. Bruckman, S. Q. Li, L. A. Lee, B. Lee, S. Pingali, P. Thiyagarajan and Q. Wang, *Langmuir*, 2007, 23, 6719.
- 19 J. Stejskal and R. G. Gilbert, *Pure Appl. Chem.* 2002, 74, 857.
- 20 Z. Zhang, Z. Wei and M. Wan, *Macromolecules*, 2002, 35, 5937; X. Lu, H. Mao, D. Chao, W. Zhang and Y. Wei, *Macromol. Chem. Phys.*, 2006, 207, 2142; H. Qiu and M. Wan, *J. Polym. Sci., Part A: Polym. Chem.* 2001, 39, 3485; H. Qiu, M. Wan, B. Matthews and L. Dai, *Macromolecules*, 2001, 34, 675; L. Zhang and M. Wan, *Nanotechnology*, 2002, 13, 750; Z. Wei, Z. Zhang and M. Wan, *Langmuir*, 2002, 18, 917; Y. Long, L. Zhang, Y. Ma, Z. Chen, N. Wang, Z. Zhang and M. Wan, *Macromol. Rapid Commun.* 2003, 24, 938; Y. Long, J. Luo, J. Xu, Z. Chen, L. Zhang, J. Li and M. Wan, *J. Phys.: Condens. Matter*, 2004, 16, 1123; H. Xia, H. S. Chan, C. Xiao and D. Cheng, *Nanotechnology*, 2004, 15, 1807; N. J. Pinto, P. L. Carrión, A. M. Ayala and M. Ortiz-Marciales, *Synth. Met.*, 2005, 148, 271; Z. Zhang, Z. Wei, L. Zhang and M. Wan, *Acta Mater.*, 2005, 53, 1373; L. Zhang and M. Wan, *Thin Solid Films*, 2005, 477, 24; H. Xia, J. Narayanan, D. Cheng, C. Xiao, X. Liu and H. S. O. Chan, *J. Phys. Chem. B*, 2005, 109, 12677.
- 21 Y. S. Yang and M. X. Wan, *J. Mater. Chem.*, 2002, 12, 897; L. Zhang and M. Wan, *Adv. Funct. Mater.*, 2003, 13, 815; L. Zhang, Y. Long, Z. Chen and M. Wan, *Adv. Funct. Mater.*, 2004, 14, 693; L. Zhang, H. Peng, Z. D. Zujovic, P. A. Kilmartin, C. Soeller and J. Travas-Sejdic, *Macromol. Chem. Phys.*, 2007, 208, 1210; Q. Sun and Y. Deng, *Mater. Lett.*, 2008, 62, 1831; Z. D. Zujovic, L. Zhang, G. A. Bowmaker, P. A. Kilmartin and J. Travas-Sejdic, *Macromolecules*, 2008, 41, 3125; P. Petrov, P. Mokreva, C. Tsvetanov and L. Terlemezyan, *Colloid Polym. Sci.*, 2008, 286, 691; Q. Sun, M. - C. Park and J. Deng, *Mater. Chem. Phys.*, 2008, 110, 276.
- 22 L. Zhang, H. Peng, C. F. Hsu, P. A. Kilmartin and Travas-Sejdic, *J. Nanotechnology*, 2007, 18, 115607; L. Zhang, H. Peng, P. A. Kilmartin, C. Soeller and Travas-Sejdic, *J. Electroanalysis* 2007, 19, 870; L. Zhang, H. Peng, J. Sui, P. A. Kilmartin, and Travas-Sejdic, *J. Curr. Appl. Phys.* 2008, 8, 312.
- 23 Z. Wei, M. Wan, T. Lin and L. Dai, *Adv. Mater.*, 2003, 15, 136.
- 24 C. Cheng, J. Jiang, R. Tang and F. Xi, *Synth. Met.*, 2004, 145, 61.
- 25 L. Zhang and M. Wan, *J. Phys. Chem. B*, 2003, 107, 6748.
- 26 J. Stejskal, P. Kratochvil and A. D. Jenkins, *Polymer*, 1996, 37, 367.
- 27 J. Kim, S. Kwon, S. H. Kim, C.-K. Lee, J. -H. Lee, S. J. Cho, H.-S. Lee, H. Ihee, *J. Am. Chem. Soc.* 2012, 134, 20573.
- 28 D. Henry, D. Tran, Y. Wang, J. M. D'Arcy and R. B. Kaner, *ACS Nano*, 2008, 2 (9), 1841.
- 29 Q. Tang, J. Wu, X. Sun, Q. Li and J. Lin, *Langmuir*, 2009, 25 (9), 5253.
- 30 Y. S. Zhao, J. Xu, A. Peng, H. Fu, Y. Ma, L. Jiang and J. Yao, *Angew. Chem., Int. Ed.* 2008, 47, 7301; X. Zhang, X. Zhang, W. Shi, X. Meng, C. Lee and S. -T. Lee, *Angew. Chem., Int. Ed.*, 2007, 46, 1525; S. M. Yoon, I. -C., Hwang, K. S. Kim and H. C. Choi, *Angew. Chem., Int. Ed.* 2009, 48, 2506.
- 31 J. Tang, X. Jing, B. Wang and F. Wang, *Synth. Met.* 1988, 24, 231; F. L. Lu, F. Wudl, M. Nowak and A. J. Heeger, *J. Am. Chem. Soc.* 1986, 108, 8311.
- 32 E. T. Kang, K. G. Neoh, K. L. Tan, *Prog. Polym. Sci.* 1998, 23, 277.
- 33 Z. M. Zhang, Z. X. Wei, M. X. Wan, *Macromolecules*, 2002, 35, 5937.
- 34 W. Li, M. Zhu, Q. Zhang and D. Chen, *Appl. Phys. Lett.* 2006, 89, 103110.
- 35 J. P. Pouget, M.E. J6zefowicz, A. J. Epstein, X. Tang and A.G. MacDiarmid, *Macromolecules*, 1991, 24, 779.
- 36 G. Louarn, S. Quillard, S. Lefrant and P.N. Prasad (Ed.), *Polymers and other Advanced Materials: Emerging Technologies and Business Opportunities*, Plenum, New York (1995), p. 317.
- 37 J. X. Huang and R. B. Kaner, *Nat. Mater.* 2004, 3, 783.
- 38 G. Ćirić-Marjanović, V. Dondur, M. Milojević, M. Mojović, S. Mentus, A. Radulović, Z. Vuković and J. Stejskal, *Langmuir*, 2009, 25 (5), 3122; B. H. Kim, J. H. Jung, J. Joo, J. Kim and H. J. Choi, *J. Korean Phy. Soc.* 2000, 36, 366.
- 39 M. Iwamoto, *J. Appl. Phys.* 1995, 77, 5314.

40 J. R. Macdonald, *Impedance Spectroscopy*, Wiley-Interscience, New York, 1987, p.66.

41 J. Frankel, *Kinetic theory of Liquids*, 1955, Dover, New York.

5

¹⁰ [A table of contents entry: Text](#)

Self-assembled and surface decorated PANI nanotubes with rectangular hollow core having high electrical and dielectric properties